A Recombinant Human RNASET2 Glycoprotein With Antitumorigenic and Antiangiogenic Characteristics

Expression, Purification, and Characterization

Patricia Smirnoff, PhD[1]
Levava Roiz, PhD[2]
Boaz Angelkovitch, MSc[2]
Betty Schwartz, PhD[1]
Oded Shoseyov, PhD[2]

[1] Institute of Biochemistry, Food Science, and Nutrition, Faculty of Agricultural, Food, and Environmental Quality Sciences, The Hebrew University of Jerusalem, Jerusalem, Rehovot, Israel.

[2] The Robert H. Smith Institute of Plant Science and Genetics in Agriculture, Faculty of Agricultural, Food, and Environmental Quality Sciences, The Hebrew University of Jerusalem, Jerusalem, Rehovot, Israel.

Address for reprints: Oded Shoseyov, PhD, The Robert H. Smith Institute of Plant Sciences and Genetics in Agriculture, Faculty of Agricultural, Food, and Environmental Quality Sciences, The Hebrew University of Jerusalem, PO Box 12, Rehovot 76100, Israel; Fax: (011) 972-8-9462283; E-mail: shoseyov@agri.huji.ac.il

Received April 4, 2006; revision received September 19, 2006; accepted September 22, 2006.

BACKGROUND. Human RNASET2 is a T_2-RNase glycoprotein encoded by the *RNASET2* gene, which is located on chromosome 6 (6q27). Deletion in 6q27 is associated with several human malignancies.

METHODS. A synthetic *RNASET2* gene that was optimized for expression in the yeast *Pichia pastoris* was designed according to the cDNA sequence and was cloned under the control of the methanol-induced promoter fused to the α-mating secretion peptide. The recombinant protein was purified from the culture supernatant of transformed *P. pastoris* through an affinity Sepharose-concanavalin A column. Actin-binding activity was examined by membrane blotting using monoclonal mouse antiactin immunoglobulin M and by cross-linking in solution to G-actin using 1-[3-(dimethylamino)propyl]-3-ethyl-carboimide methiodide. The antiangiogenic activity of RNASET2 (from 0.5 μM to 10 μM) was assessed by a human umbilical vein endothelial (HUVE) cell assay in the presence of 1 μg/mL angiogenin, basic fibroblast growth factor (bFGF), or recombinant human vascular endothelial growth factor (VEGF). Cell colony formation was examined in human colon HT29 cancer cells to assess the antitumorigenic activity of RNASET2 or the enzymatic-inactivated RNASET2 (EI-RNASET2) (1 μM each). In an athymic mouse xenograft model, LS174T human cancer cells were injected subcutaneously. When tumors were palpable, the mice were treated for 3 weeks with RNASET2 (1 mg/kg), paclitaxel (10 mg/kg or 15 mg/kg), or a combination of the 2 drugs.

RESULTS. The recombinant RNASET2 was identified as a 27-kilodalton glycoprotein that possessed the ability to bind actin in vitro. RNASET2 significantly inhibited clonogenicity in HT29 cells. EI-RNASET2 produced a similar effect, suggesting that its antitumorigenic activity is unrelated to its RNase activity. In HUVE cells, RNASET2 inhibited angiogenin-, bFGF-, and VEGF-induced tube formation in a dose-dependent manner. In athymic mice, RNASET2 inhibited the development of an LS174T-derived xenograft by 40%. A synergistic effect was obtained with combined RNASET2 and paclitaxel treatments.

CONCLUSIONS. The current results suggested that RNASET2 represents a new class of antitumorigenic and antiangiogenic drugs, and the findings of this study emphasize the advantage of using agents like RNASET2 in combined therapy. ***Cancer* 2006;107:2760–9.** © *2006 American Cancer Society.*

KEYWORDS: antiangiogenic, actin-binding, colon cancer, paclitaxel, RNASET2.

RNases currently are the focus of much attention because of their newly discovered activities and applications, particularly in cancer biology.[1,2] RNases of the T2 family are distributed widely, from viruses to mammals, and play a role in a variety of biologic functions.[1,3] During the last few years, considerable effort has been

DOI 10.1002/cncr.22327
Published online 15 November 2006 in Wiley InterScience (www.interscience.wiley.com).

devoted in our laboratory to a unique T2-ribonuclease, ACTIBIND, which is produced by the mold *Aspergillus niger*.[4] We have observed that ACTIBIND is a glycoprotein that can bind actin in vitro in a molar ratio of 1:2, respectively. In plant and mammalian cells, it accelerates the formation of cross-links between actin filaments and, thus, leads to disruption of the intracellular actin network and, consequently, to cell growth and cell-migration arrest (unpublished data). These events play a key role in cancer and angiogenic cells,[5] and, accordingly, ACTIBIND was identified as an effective antiangiogenic and anticarcinogenic agent.[6] In human umbilical vein endothelial (HUVE) cells, ACTIBIND inhibited tube formation induced by different growth factors, including angiogenin, basic fibroblast growth factor (bFGF), and vascular endothelial growth factor (VEGF). In nude mice, ACTIBIND inhibited the development of human colon cancer HT29 xenografts. In rats, ACTIBIND exerted preventive and therapeutic effects on developing colonic tumors induced by dimethylhydrazine. In rat colon tumors, ACTIBIND also caused a significant reduction in the degree of tumor vascularization.[6]

In the human genome, deletion of a telomeric region in the long arm of chromosome 6 (6q27) has been considered to be associated with a variety of solid neoplasms, including carcinomas of the ovary,[7,8] breast,[9–11] uterus,[12] stomach,[13] liver,[14] colon/rectum,[15] kidney,[16] and parathyroid gland[17] as well as melanoma[18] and hematologic malignancies, like non-Hodgkin B-cell lymphoma[19] and acute lymphoblastic leukemia.[20] The 6q27 region was mapped, and investigators found that it contained a tumor suppressor gene formerly known as *RNase6PL* and recently renamed *RNASET2*. This gene is present in a single copy in the genome; of 28,751 base pairs (bp) of the full gene, only 719 bp (split into in 9 exons) form the open reading frame.[21–24] Both in primary ovarian tumors and in ovarian tumor cell lines, *RNASET2* gene expression is reduced significantly, although it is not necessarily mutated.[21,24] The putative protein (National Center for Biotechnology Information [NCBI] GeneInfo no. [gi] 30354311) encoded by this gene shares homology with the RNase T2 family.[21,24] Amino acid sequence alignment between ACTIBIND (NCBI gi 71064123) and the putative *RNASET2*-encoded protein showed 34% identity and 52% homology. In ovarian cancer cell lines, transfection with *RNASET2* caused a reduction in tumorigenicity[24] and in the ability to metastasize in nude mice xenografts.[23]

The similarity between RNASET2 and ACTIBIND raised interest in studying the antitumorigenic effects of human T2-RNase. In the current study, we cloned the *RNASET2* gene into the yeast *Pichia pastoris* and expressed the recombinant protein. The RNASET2 protein was purified and found to bind actin. In vitro assays and animal experiments demonstrated the antiangiogenic and antitumor effects of RNASET2.

MATERIALS AND METHODS

Chemicals, Drugs, and Supplies

The enhanced chemiluminescence (ECL) Western blot detection system was from Amersham Pharmacia Biotech, Ltd. (Buckinghamshire, U.K.); Matrigel was from Becton-Dickinson (Bedford, MA); Dulbecco minimum Eagle medium (DMEM), M199 medium, fetal calf serum (FCS), glutamine, and antibiotic-antimycotic solution were from Biological Industries (Bet Haemek, Israel); endothelial cell growth factor (ECGF) was from Biomedical Technologies Inc. (Stoughton, MA); monoclonal mouse antiactin-immunoglobulin M (IgM) and horseradish peroxidase (HRP)-conjugated goat anti-mouse IgM were from Calbiochem-Novabiochem Company (San Diego, CA); the *RNASET2* gene was synthesized by GenArt GmbH (Regensburg, Germany); pPIC9K was from Invitrogen (San Diego, CA); paclitaxel was from Mead Johnson, Bristol-Myers Squibb Company (Princeton, NJ); bFGF was from Promega (Madison, WI); recombinant human VEGF was from Protein Laboratories (Rehovot, Israel); recombinant human angiogenin was from R&D Systems, Inc. (Minneapolis, MN); agarose, concanavalin A immobilized on 4% cross-linked beaded agarose, G-actin, 1-[3-(dimethylamino)-propyl]-3-ethyl-carboimide methiodide (EDC), methyl α-D mannopyranoside, and yeast RNA were from Sigma-Aldrich Company (St. Louis, MO).

Cloning Human RNASET2

A synthetic *RNASET2* gene that was optimized for expression in Pichia pastoris was designed according to the complementary DNA (cDNA) sequence and cloned into the plasmid pCR-Script Amp. The fragment of 719 bp resulting from *Eco*RI and *Not*I digestion was subcloned into the *Eco*RI/*Not*I sites of pPIC9K and transformed into *Escherichia coli* strain DH5α, as described previously.[25] Expression in *P. pastoris* strain GS115 (*his4* mutant) was carried out according to the manufacturer's protocol (*Pichia* expression kit; Invitrogen, Life Technologies). The yeast was cultivated in 25 mL of medium containing 1% yeast extract; 2% peptone; 100 mM potassium phosphate, pH 6.0; 4×10^{-5}% biotin; and 1% glycerol (BMG medium) overnight at 30°C with orbital shaking. The cells were centrifuged further and transferred to a another medium, which was the same as BMG but contained 1% methanol in place of glyc-

erol, for 6 days under the conditions used for protein expression.

Purification of the Recombinant RNASET2

The yeast growth medium was centrifuged at 4000g for 10 minutes at 10°C to remove any cell debris and the supernatant was passed sequentially through 0.45-μm and 0.2-μm filters. The filtrate was brought to pH 7.4 with 1 M Tris and 6 M NaOH, centrifuged as described above, and refiltered. Then, the filtrate was incubated overnight at 4°C under continuous rotation with concanavalin A immobilized on 4% cross-linked, beaded agarose in equilibration buffer (20 mM Tris-HCl, pH 7.4; 500 mM NaCl; 1 mM $CaCl_2$; 1 mM $MgCl_2$; and 1 mM $MnCl_2$). A column (3.5 cm × 1.3 cm) was built with the beads and washed with the equilibration buffer. Because *P. pastoris* uses mannose as a keystone for protein glycosylation, the RNASET2 was released with 500 mM methyl α-D mannopyranoside. The eluate was dialyzed intensively against double-distilled water and lyophilized. The isolated glycoprotein was analyzed by 12.5% Tricine-sodium dodecyl sulfate-polyacrylamide gel electrophoresis (SDS-PAGE).[26]

RNase Activity Assays

The RNase activity assay was performed as described previously with modifications.[4,27] Samples of 50 μL were added to 50 μL of 100 mM sodium acetate buffer (pH 4.5) that contained 4 mg/mL yeast RNA. Blank tubes were prepared in the same way, except that the RNASET2 was replaced with buffer. The reaction mixture was incubated for 30 minutes at 50°C; then, 50 μL of stop mixture (0.75% weight/volume uranyl sulfate in 25% weight/volume perchloric acid) were added. The reaction mixture was cooled on ice for 5 minutes and centrifuged at 15,000 g for 5 minutes. The supernatant fluid was diluted 8-fold with distilled water, and absorbance was determined at 260 nanometers (nm). Enzymatic-inactivated (EI)-RNASET2 was obtained after autoclaving at 120°C (120 kPa) for 30 minutes (ie, until RNase activity was undetectable).

A zymogram for RNase activity was performed as modified from Roiz et al.[4] Samples of 5 μL were placed over a plate that contained 10 mL of 0.1% yeast RNA and 0.8% agarose in 20 mM sodium acetate and were incubated at 37°C for 30 minutes. Then, the agarose plate was stained with 0.02% (weight/volume) Toluidine blue in water. RNase activity was visualized as a bright area on a blue background.

Clonogenic Assay

The colony-formation assay was performed essentially as described previously[28] with minor modifications. Human colon cancer HT29 cells were grown in 50-mL flasks (10^5 cells/flask) in 7 mL DMEM supplemented with 10% FCS, 1% glutamine and 1% antibiotic-antimycotic solution in the presence or absence of 1 μM RNASET2 or EI-RNASET2. The cells were incubated at 37°C in a humidified atmosphere containing 5% carbon dioxide, and the growth medium was changed 24 hours after cell implantation. After another 24 hours, the cells were seeded in 96-well, flat-bottomed microtiter plates (10^3 cells per well) in 200 μL medium in the presence or absence of 1 μM RNASET2 or EI-RNASET2 and incubated for 5 days. The colonies were then fixed with 5% formaldehyde, 60% ethanol, and 5% acetic acid in water for microscopy observations. In each treatment, colonies that contained at least 100 cells were counted. Six individual determinations were performed for each treatment.

HUVE Cell Angiogenesis Assay

Freshly isolated HUVE cells were maintained in M199 medium supplemented with 20% FCS, 1% glutamine, 1% antibiotic-antimycotic solution, 0.02% ECGF, and 50 U/100 mL heparin, as described previously.[29] Then, the cells were plated (14×10^3 cells per well) in a 96-well plate coated with growth factor-depleted Matrigel in 100 μL M199 medium that contained 5% FCS and 0.005% ECGF supplemented with recombinant human angiogenin, bFGF, or recombinant human VEGF to a final concentration of 1 μg/mL each. RNASET2 (0.5 μM, 1 μM, 5 μM, or 10 μM final concentration) or phosphate-buffered saline (PBS) was added. After incubation overnight, the plates were photographed, and the extent of tube formation was assessed. Five individual determinations were performed for each treatment.

Binding of RNASET2 to Actin

Membrane blotting

RNASET2, ACTIBIND, bovine serum albumin (BSA) (as a negative control), or G-actin (positive control) was blotted directly onto nitrocellulose membrane using a SlotBlot (Hoefer Scientific Instruments, San Francisco, CA). The membrane was blocked overnight at 4°C with 5% (weight/volume) skim milk in PBS that contained 0.25% Tween 20 (PBST) and was washed twice for 10 minutes each with 1% milk in PBST. Then, the membrane was equilibrated with freshly prepared Buffer G (2 mM Tris-HCl, pH 8.0; 0.2 mM $CaCl_2$, and 0.2 mM adenosine triphosphate) for 10 minutes at room temperature and subsequently incubated overnight at 4°C with 5 μg/mL G-actin in Buffer G. The membrane was washed 3 times for 10 minutes each at room temperature with

1% milk in PBST that contained 0.2 mM $CaCl_2$, probed for 1 hour against monoclonal mouse antiactin-IgM (20 μg/mL in 2 mM Tris-HCl, pH 7.4, containing 0.2 mM $CaCl_2$), washed again 3 times for 10 minutes each in PBST with 0.2 mM $CaCl_2$, and reacted against 0.1 μg/mL HRP-conjugated goat antimouse IgM. Signals were detected with an ECL Western Blot Detection System.

Binding in solution

The assay was done as described by Hu et al.[30] Actin (10 μg) was mixed with RNASET2 or EI-RNASET2 (20 μg each) in 15 μL Buffer G. The mixture was incubated for 30 minutes at room temperature; then, EDC was added to a final concentration of 10 mM. After another 30-minute incubation at room temperature, the cross-linked complex was run on 12.5% Tricine SDS-PAGE gels. Proteins were visualized by Coomassie blue staining or by Western blot analysis using mouse antiactin-IgM as described above.

Animal Studies in Xenograft Model

Viable human colon cancer LS174T cells were injected subcutaneously (5×10^5 cells/100 μL per mouse) into the left hip of female athymic mice aged 5 or 6 weeks (Athymic Nude/nu; Harlan, Rehovot, Israel). When the tumor diameter reached 5 mm to 7 mm (approximately 2 weeks after implantation), the mice were treated with RNASET2 (1 mg/kg) injected into the peritoneal cavity (intraperitoneally), with paclitaxel (10 mg/kg or 15 mg/kg) injected into the tail vein (intravenously), or with a combination of the 2 drugs. RNASET2 was injected every 2 days for 3 weeks; paclitaxel at a dose of 10 mg/kg was injected 3 times a week for 3 weeks; paclitaxel at a dose of 15 mg/kg was injected 4 times every 2 days starting from the second week of the experiment. Control mice received PBS every 2 days throughout the experimental period. The mice were maintained on a normal diet that was provided ad libitum under pathogen-free conditions. Tumors were measured with calipers 3 times per week. Tumor size (mm^3) was evaluated by measuring the 2 greatest perpendicular dimensions with Vernier calipers and using the formula $1/2LW^2$,[31] in which L is the greatest dimension, and W is the dimension perpendicular to L, and the results are presented as mean values. The experiments were terminated 21 days after the initial treatment. The mice were killed, and tumors were taken for histopathologic examination. In each median tumor cross section, the blood vessels were counted, and their areas were analyzed with Image J (NIH) software. Relative area (percentage) was calculated as the ratio between total blood-vessel area and tumor-section area (n = 5 tumors; 3 microscopic fields of each). All animal experiments were approved by the Ethics Committee for Animal Experimentation, Faculty of Agricultural, Food, and Environmental Quality Sciences, the Hebrew University of Jerusalem, Israel.

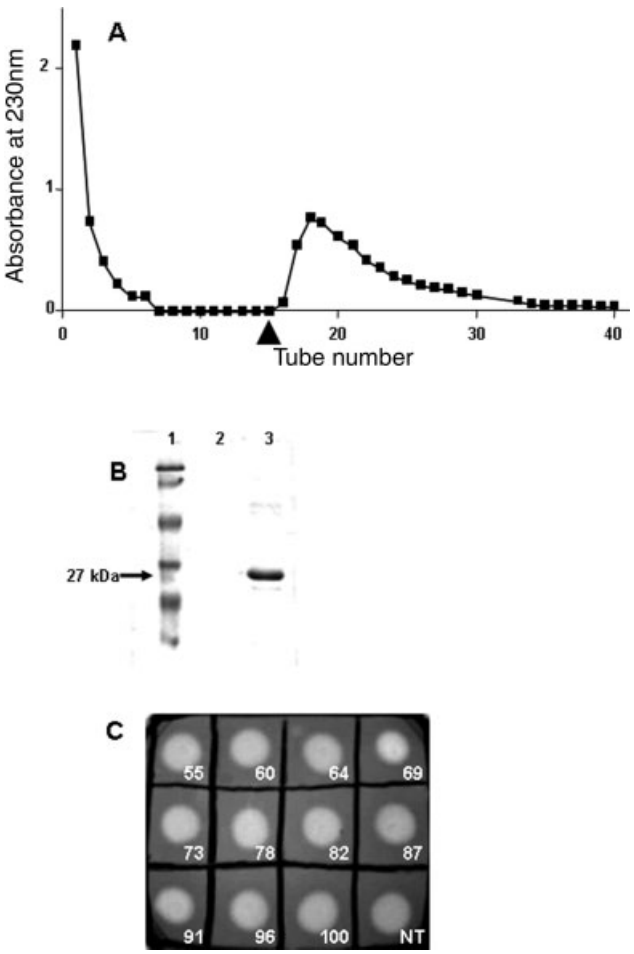

FIGURE 1. (A) Purification of human recombinant RNASET2 by affinity chromatography. The growth medium of *Pichia pastoris* was passed through concanavalin A immobilized on a 4% cross-linked, beaded agarose column. The glycoprotein was eluted after addition of 500 mM methyl α-D mannopyranoside (arrowhead). (B). Protein analysis on 12.5% SDS-PAGE. Lane 1, molecular markers; Lane 2, fractions collected with equilibration buffer; Lane 3, RNASET2. (C). Zymogram for RNase activity. Samples of human recombinant RNASET2 were heated for 10 minutes at a range of temperatures (from 55°C to 100°C); then, 5 μL of each were placed on an agarose plate containing yeast RNA. The bright circles indicate that RNase activity was retained, even at boiling point. Each number represents a temperature (°C). NT indicates not treated.

Statistical Analysis

Means were compared by using an analysis of variance. Differences were considered statistically significantly at $P < .05$.

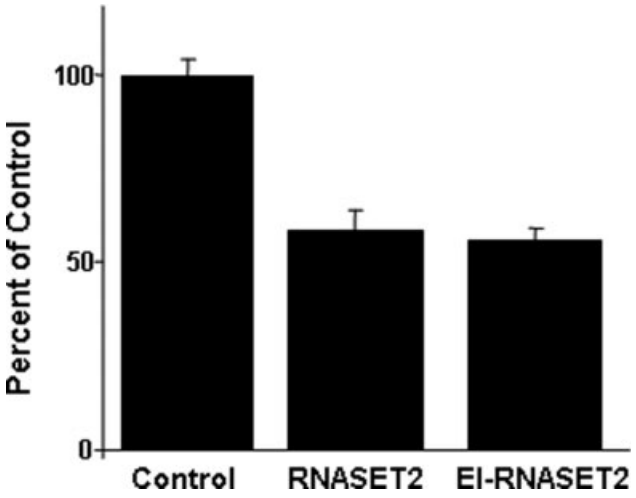

FIGURE 2. The effect of RNASET2 and EI-RNASET2 (1 μM each) on clonogenicity in colon cancer HT29 cells. The number of colonies (percent of control) was significantly lower in RNASET2- and in EI-RNASET2-treated cells ($P < .01$) relative to controls (n = 6 for each treatment).

RESULTS

The synthetic *RNASET2* gene was ligated into the pPIC9K plasmid downstream to α-mating factor secretion signal peptide and expressed by the yeast *P. pastoris*.[32,33] The recombinant RNASET2 was affinity purified by concanavalin A immobilized on a 4% cross-linked, beaded agarose column (Fig. 1A); and a pure RNase-active glycoprotein at the expected size of 27 kilodaltons (kDa) (Fig. 1B) was eluted, indicating accurate folding during synthesis of the recombinant RNASET2 protein. The recombinant RNASET2 maintained its thermostability and RNase activity, even at boiling point (Fig. 1C). These properties are typical of T2-RNase family members. Therefore, autoclave treatment was required to abolish RNase activity completely.

The biologic activity of the RNASET2 was analyzed by in vitro and in vivo assays. The antitumorigenic effect was assessed by determining the ability to inhibit cancer cell colony formation. In HT29 can-

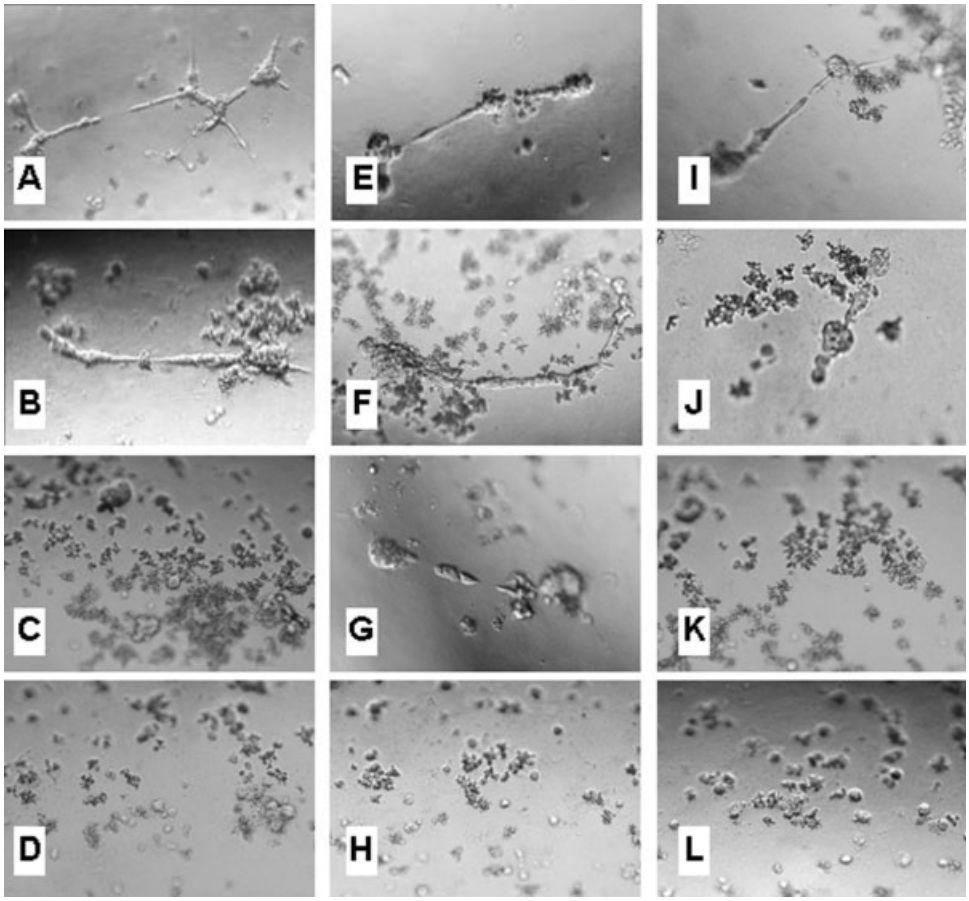

FIGURE 3. HUV cell tube formations on Matrigel were induced by angiogenin (A-D), bFGF (E-H), and VEGF (I-L). Controls (A, E, and I), in 1 μM RNASET2 (B, F, and J), in 5 μM RNASET2 (C, G, and K), 10 μM RNASET2 (D, H, and L). Tube formation was inhibited by RNASET2 in a dose-dependent manner and reached total arrest at 5 μM with angiogenin and VEGF and at 10 μM with bFGF (n = 5 for each treatment).

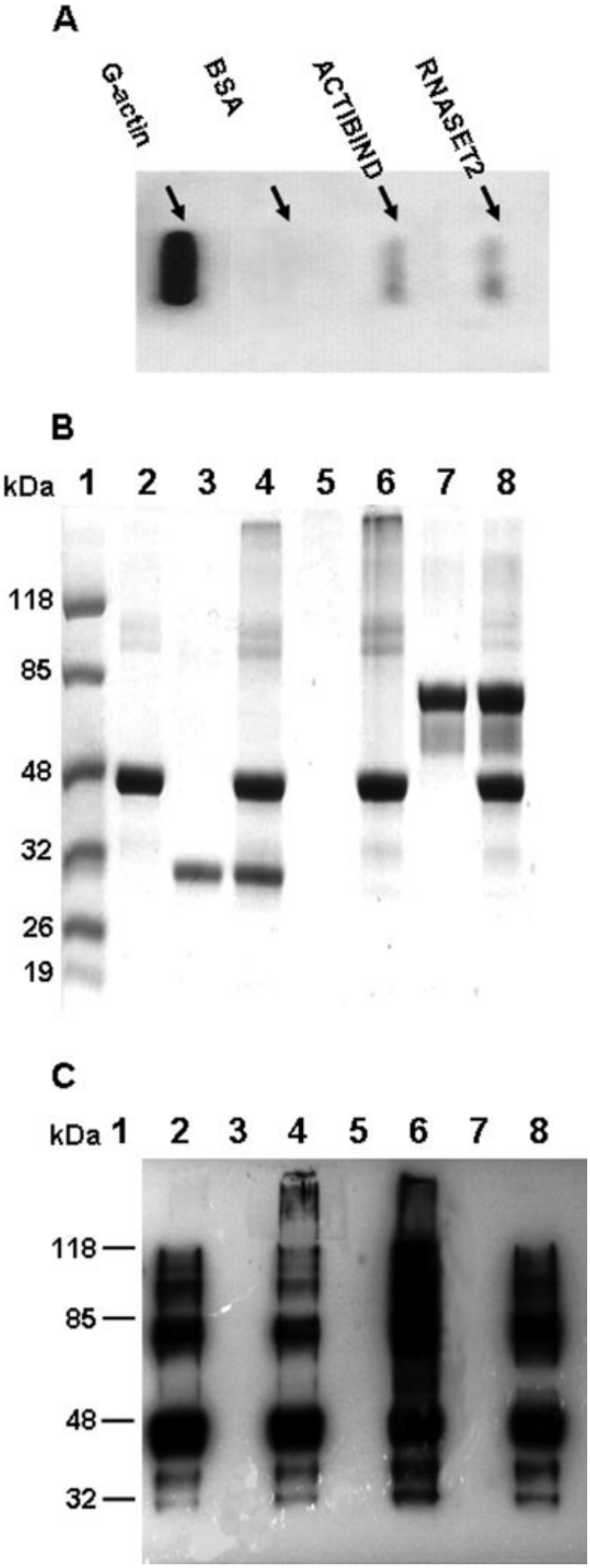

cer cells, RNASET2 and EI-RNASET2 significantly reduced the rate of colony formation to 59% and 56%, respectively, compared with controls ($P < .01$) (Fig. 2).

The antiangiogenic effect of RNASET2 was assessed by HUVE cell tube formation on Matrigel. We observed that RNASET2 inhibited angiogenin- and VEGF-induced tube formation in a dose-dependent manner (Fig. 3), reaching total arrest at 5 μM. With bFGF, total arrest was reached at 10 μM.

Binding of RNASET2 to actin was analyzed by ligand blotting. We observed that actin was bound to membrane-immobilized RNASET2 and to ACTIBIND, but not to BSA (Fig. 4A). The binding of RNASET2 to actin also was investigated by cross-linking followed by gel electrophoresis. Coomassie-blue staining revealed that, when RNASET2 was mixed with actin, a band at a high molecular weight that hardly penetrated the running gel appeared, suggesting the formation of a super-complex between RNASET2 and actin (Fig. 4B, Lane 4). Although the denaturated EI-RNASET2 was not observed with Coomassie blue (Fig. 4B, Lane 5), a high-molecular-weight complex with actin (Fig. 4B, Lane 6) was obtained similarly to the native RNASET2. No complex was observed when actin was mixed with BSA under the same conditions (Fig. 4B, Lane 8). These results were validated by Western blot analysis with antiactin antibody (Fig. 4C). Additional bands that contained only actin and that migrated with higher molecular mass (Fig. 4C, Lane 2) most likely are the results of actin oligomerization.[34,35]

Using the xenograft athymic mouse model, we investigated the ability of RNASET2 to affect the growth rate of LS174T-derived carcinoma (Fig. 5). Each of the individual treatments (RNASET2 or paclitaxel) led to approximately 40% inhibition of tumor development compared with controls. Conversely,

FIGURE 4. Actin-binding activity assays. (A) Membrane blotting: Proteins were blotted onto a nitrocellulose membrane, and actin-binding capability was evaluated after overnight incubation with 10 μg/mL actin. Proteins bound to actin were evidenced subsequent to reaction with antiactin followed by HRP-conjugated secondary antibody. (B,C) Binding in solution. Actin (10 μg) was mixed with 20 μg RNASET2, EI-RNASET2, or BSA (as a control) in 15 μL Buffer G. After incubation for 30 minutes at room temperature, the mixture was cross-linked for 30 minutes with EDC and analyzed by 12.5% SDS-PAGE. Lane 1, molecular markers; Lane 2, actin; Lane 3, RNASET2; Lane 4, RNASET2 and actin; Lane 5, EI-RNASET2; Lane 6, EI-RNASET2 and actin; Lane 7, BSA; Lane 8, BSA and actin. Gel was stained with Coomassie blue (B) or was immunoblotted using mouse IgM (C).

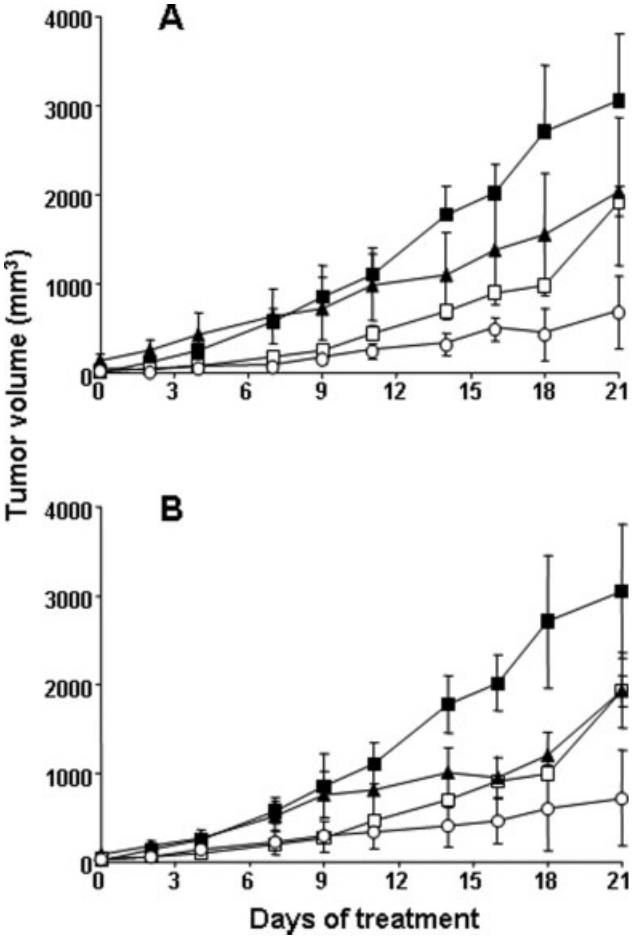

FIGURE 5. The effect of RNASET2 on LS174T-derived colon cancer cells implanted in nude mice. The cells were injected subcutaneously (5×10^5 cells per mouse) into the left hip. When the tumor diameter reached 5 mm to 7 mm, the mice were distributed randomly ($n = 6$) and were treated for 3 weeks with 1 mg/kg RNASET2, (every 2 days $\times$ 3 weeks intraperitoneally; open squares), with paclitaxel (intravenously; solid triangles), or with a combination of the 2 drugs according to their respective schedules (open circles). (A) Mice treated with 10 mg/kg paclitaxel 3 times per week for 3 weeks. (B) Mice treated with 15 mg/kg paclitaxel 4 times every 2 days starting from the second week of the experiment. Control mice received PBS every 2 days $\times$ 3 weeks (intraperitoneally; solid squares). The combined treatments show a significant ($P \leq .005$) synergistic effect compared with the control or with each of the individual treatments. Each bar represents the standard error of the mean.

combination treatments of RNASET2 with paclitaxel resulted in approximately 80% inhibition ($P \leq .005$) compared with controls (Fig. 5A,B), thus showing a synergistic effect.

Histologic analysis demonstrated the effect of the different treatments on tumor blood vessels. In control mice, a wide invasive area with LS174T cancer cells was observed and was accompanied by large blood vessels (Fig. 6A). The endothelial cells were intact, and tumor cells were attached to the blood vessels (Fig. 6D). In mice that were treated with RNASET2 (Fig. 6B) or with RNASET2 and paclitaxel (Fig. 6C), cancer cells were concentrated surrounding small blood vessels. In RNASET2-treated mice (Fig. 6E), blood cells infiltrated through the endothelium from the blood vessels, and tumor cells were detached from the endothelium. In mice that were treated with RNASET2 and paclitaxel (Fig. 6F), a substantial loss of endothelial structure was observed. Furthermore, the effect of RNASET2 on angiogenesis was determined in the median tumor cross-sections. Both RNASET2 treatment and the combination treatment with paclitaxel significantly reduced the number of blood vessels per tumor by 49% ($P < .005$) and 44%, ($P < .01$), respectively, relative to controls. In addition, a 68% reduction in total blood vessel area per tumor section ($P < .001$) was observed for both treatments compared with controls.

DISCUSSION

In this article, we report on the expression of RNASET2 glycoprotein in *P. pastoris* from an optimized synthetic human *RNASET2* gene. The recombinant RNASET2 was purified on a concanavalin A-immobilized, cross-linked, beaded agarose column (Fig. 1). In vitro assays showed that RNASET2 bound actin (Fig. 4). The antiangiogenic effect of RNASET2 was demonstrated by its inhibition of angiogenin-, bFGF-, and VEGF-induced HUVE cell tube formation in vitro in a dose-responsive manner (Fig. 3). The antitumorigenic effect of RNASET2 was demonstrated by its ability to reduce significantly the clonogenic ability of cancer cells (Fig. 2).

If the antitumorigenic effect was a result of RNA degradation and protein biosynthesis depletion, then EI-RNASET2, which shows no RNase activity, would be ineffective. However, the EI-RNASET2 possessed anticlonogenic (Fig. 2) and actin-binding (Fig. 3) activities, similar to the nontreated RNASET2. We previously reported that the anticarcinogenic and antiangiogenic effects of the fungal ACTIBIND are not related to its ribonuclease activity.[6] Our findings are supported by those of Acquati et al.,[22,23] who reported that a double point mutation targeted to the putative ribonuclease catalytic sites did not affect RNASET2-mediated tumor suppression and metastasis, suggesting that RNase activity is not a prerequisite for its antitumorigenic effect. Alternatively, the antitumorigenic activity of the aforementioned members of the RNase T2 family may be associated with actin binding rather

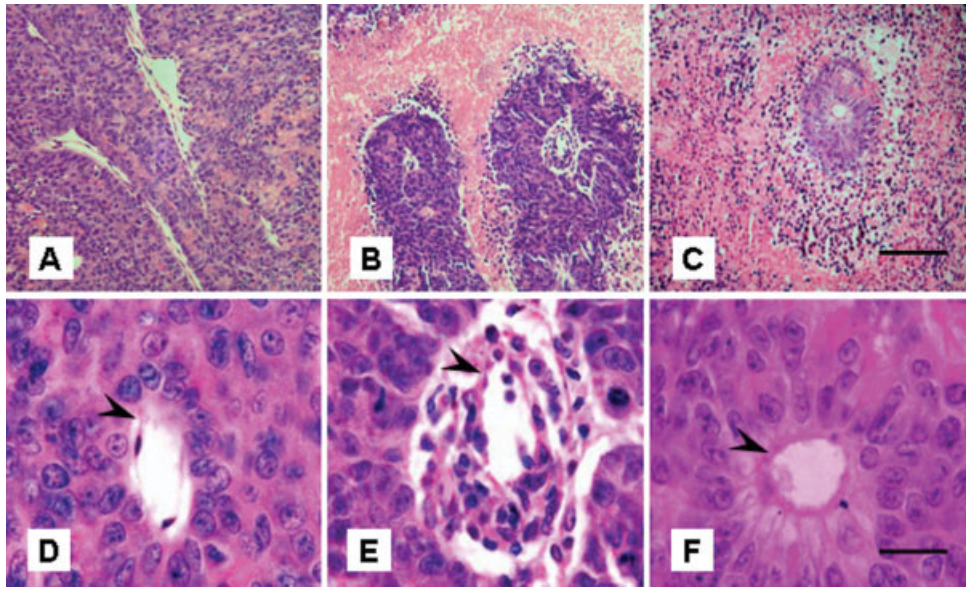

FIGURE 6. Paraffin sections of LS174T-derived xenografts in nude mice after hematoxylin and eosin staining. Controls (A and D), RNASET2-treated tumors (B and E), and tumors treated with both RNASET2 and paclitaxel (C and F). In control mice, a wide, invasive area with LS174T cancer cells is observed accompanied by large blood vessels (A). Magnification of blood vessels shows cancer cells reaching up to the endothelial cells (D). In mice treated with RNASET2 (B) and with RNASET2 plus paclitaxel (C), cancer cells are concentrated surrounding small blood vessels. In RNASET2-treated tumors, the blood cells infiltrate out through the endothelium, and the tumor cells detach from the blood vessel (E). In mice treated with RNASET2 and paclitaxel, the endothelium structure is destroyed (F). Scale bar = 50 μm in A, B, and C; 10 μm in D, E. and F.

than RNase activity. Simm et al.[36] reported that bovine seminal-RNase, a member of the RNase A family, also binds actin in vitro. The biologic function of this RNase includes antitumor and immunorepressive activities.[37,38] In cancer cells, the structure of the actin network is related directly to malignancy potential, because it determines cell motility.[5] Furthermore, in endothelial cells, it has been demonstrated that surface actin is a receptor for angiogenin, thus playing a critical role in angiogenesis.[30,39–41] The mechanism by which RNASET2 binds to cell-surface actin, leading to antitumorigenic activity, deserves a more in-depth investigation.

The antitumorigenic and antiangiogenic effects of RNASET2 also were demonstrated in vivo in a xenograft model. In athymic mice, RNASET2 injected intraperitoneally every 2 days significantly inhibited viable human colon cancer LS174T-derived xenograft development (Fig. 5), which is known as a hypervascular model.[42] In addition, RNASET2 affected the histology of tumors and blood vessels (Fig. 6). Furthermore, reductions in the number of blood vessels per tumor and in blood vessel size were observed. Acquati et al.[24] reported that transfection of *RNASET2* cDNA into ovarian cancer cells reduced their tumorigenicity in nude mice.[22] In contrast, Liu et al.[42] reported that transfection of the same gene into ovarian cancer cells did not result in suppression of clonogenicity. A possible explanation for the latter result is that, in the study by Liu et al., the RNASET2 cDNA was fused to an HA epitope tag at the C-terminus, which may have affected the ability of the encoded protein to be secreted. Consequently, it did not have access to its natural receptor on the target cell surface.

The resistance of many tumors to conventional therapy has led to attempts to develop novel and more effective strategies to improve anticancer agents. In the current study, a synergistic effect was obtained with paclitaxel at low clinical doses (15 mg/kg and 10 mg/kg) and in 2 different regimes, emphasizing the advantage of concomitant use of RNASET2 in combined therapy. These results are related to the study reported by Fujii et al.[43] in a human LS174T colon cancer xenograft model, in which combined therapy with paclitaxel/thalidomide inhibited tumor growth and angiogenesis in mice synergistically. The practice of combining chemotherapy with antiangiogenic drugs is on the rise for the treatment of malignancies with greater sensitivity and less toxicity.[43–46] Most recently, a large Phase III study has provided unequivocal evidence that VEGF inhibition, using bevacizumab (Avastin) in combination with chemotherapy, can provide substantial clinical benefits, in-

cluding increased survival, in patients with metastatic colorectal carcinoma.[47] Bevacizumab is the first anti-angiogenic agent to be approved by the U.S. Food and Drug Administration for cancer therapy.[47–49]

The major advantage of human RNASET2 arises from its potential to be well-recognized by the human body and to be tolerated with only minor (if any) side effects. Our current data also strengthen the idea that combining RNASET2 with conventional chemotherapy may be the basis for future anticancer therapy.

REFERENCES

1. Irie M, Ohgi K. Ribonuclease T2. *Methods Enzymol*. 2001;341:42–55.
2. Schein CH. From housekeeper to microsurgeon: the diagnostic and therapeutic potential of ribonucleases. *Nature Biotech*. 1997;15:529–536.
3. Deshpande RA, Shankar V. Ribonucleases from T2 family. *Crit Rev Microbiol*. 2002;28:79–122.
4. Roiz L, Ozeri U, Goren R, Shoseyov O. Characterization of *Aspergillus niger* B-1 RNase and its inhibitory effect on pollen germination and pollen tube growth in selected tree fruit. *J Am Soc Hort Sci*. 2000;125:9–14.
5. Janmey PA, Chaponnier C. Medical aspects of the actin cytoskeleton. *Curr Opin Cell Biol*. 1995;7:111–117.
6. Roiz L, Smirnoff P, Bar-Eli M, Schwartz B, Shoseyov O. Actibind: an actin-binding fungal T_2-RNase with antiangiogenic and anticarcinogenic characteristics. *Cancer*. 2006;106:2295–2308.
7. Cooke IE, Shelling AN, Le Meuth VG, Charnock ML, Ganesan TS. Allele loss on chromosome arm 6q and fine mapping of the region at 6q27 in epithelial ovarian cancer. *Genes Chromosomes Cancer*. 1996;15:223–233.
8. Saito S, Saito H, Ko S, et al. Fine-scale deletion mapping of the distal long arm of chromosome 6 in 70 human ovarian cancers. *Cancer Res*. 1992;52:5815–5817.
9. Develee P, van Vliet M, van Sloun Kuipers N, Hermans J, Pearson P, Cornelisse C. Allelotype of human breast carcinoma: a second major site for loss of heterozygosity is on chromosome 6q. *Oncogene*. 1991;6:1705–1711.
10. Theile M, Seitz S, Arnold W, et al. A defined chromosome 6q fragment (at D6S310) harbors a putative tumor suppressor gene for breast cancer. *Oncogene*. 1996;13:677–685.
11. Tibiletti MG, Sessa F, Bernasconi B, et al. A large 6q deletion is a common cytogenetic alteration in fibroadenomas, pre-malignant lesions, and carcinomas of the breast. *Clin Cancer Res*. 2000;6:1422–1431.
12. Chappell S, Walsh T, Walker R, Show J. Loss of heterozygosity at chromosome 6q in preinvasive and early invasive breast carcinomas. *Br J Cancer*. 1997;75:1324–1329.
13. Queimado L, Seruca R, Costa-Pereira A, Castedo S. Identification of two distinct regions of deletion at 6q in gastric carcinoma. *Genes Chromosomes Cancer*. 1995;14:28–34.
14. De Souza AT, Hankins GR, Washington MK, Fine RL, Orton TC, Jirtle RL. Frequent loss of heterozygosity on 6q at the mannose 6-phosphate/insulin-like growth factor II receptor locus in human hepatocellular tumors. *Oncogene*. 1995;10:1725–1729.
15. Honchel R, McDonnell S, Schaid D, Thibodeau S. Tumor necrosis factor-alpha allelic frequency and chromosome 6 allelic imbalance in patients with colorectal cancer. *Cancer Res*. 1996;56:145–149.
16. Morita R, Saito S, Ishikawa J, et al. Common region of deletion on chromosomes 5q, 6q, and 10q in renal cell cancer. *Cancer Res*. 1991;51:5817–5820.
17. Tahara H, Smith AP, Gas RD, Cryns VL, Arnold A. Genomic localization of novel candidate tumor suppressor gene loci in human parathyroid adenomas. *Cancer Res*. 1996;56:599–605.
18. Millikin D, Meese E, Vogelstein B, Witkowski C, Trent J. Loss of heterozygosity for loci on the long arm of chromosome 6 in human malignant melanoma. *Cancer Res*. 1991;51:5449–5453.
19. Gaidano G, Hauptschein RS, Parsa NZ, et al. Deletions involving two distinct regions of 6q in B-cell non-Hodgkin lymphoma. *Blood*. 1992;80:1781–1787.
20. Hayashi Y, Raimondi S, Look T, et al. Abnormalities of the long arm of chromosome 6 in childhood acute lymphoblastic leukemia. *Blood*. 1990;76:1626–1630.
21. Trubia M, Sessa L, Taramelli R. Mammalian Rh/T2/S-glycoprotein ribonuclease family genes: cloning of a human member located in a region of chromosome 6 (6q27) frequently deleted in human malignancies. *Genomics*. 1997;42:342–344.
22. Acquati F, Morelli C, Cinquetti R, et al. Cloning and characterization of a senescence inducing and Class II tumor suppressor gene in ovarian carcinoma at chromosome region 6q27. *Oncogene*. 2001;20:980–988.
23. Acquati F, Possati L, Ferrante L, et al. Tumor and metastasis suppression by the human RNASET2 gene. *Int J Oncol*. 2005;26:1159–1168.
24. Acquati F, Nucci C, Bianchi M, Taramelli R. Molecular cloning, tissue distribution, and chromosomal localization of the human homolog of the R2/Th/Stylar ribonuclease gene family. *Methods Mol Biol*. 2001;160:87–101.
25. Ausubel FM, Brent R, Kingston R, et al. Current Protocols in Molecular Biology. New York: John Wiley & Sons, Inc.; 1998.
26. Laemmli UK. Cleavage of structural proteins during the assembly of the head of bacteriophage T4. *Nature*. 1970;227:680–685.
27. Worthington Biochemical Corporation. *Worthington Enzyme Manual*: enzyme, enzyme reagents, related biochemicals. 1st edition. Freehold, NJ: Worthington Biochemical Corporation, 1972.
28. Lee I, Lee YH, Mikulski SM, Lee J, Covone K, Shogen K. Tumoricidal effects of onconase on various tumors. *J Surg Oncol*. 2000;73:164–171.
29. Ponoe ML. In vitro Matrigel angionesis assays. In: Murray JC, editor. Methods in Molecular Medicine. Volume 46: Angiogenesis Protocols. New York: Totowa Humana Press; 2001:205–209.
30. Hu GF, Strydom DJ, Fett JW, Riordan JF, Vallee BL. Actin is a binding protein for angiogenin. *Proc Natl Acad Sci USA*. 1993;90:1217–1221.
31. Bullard DE, Schold SC Jr, Bigner SH, Bigner DD. Growth and chemotherapeutic response in athymic mice of tumors arising from human glioma-derived cell lines. *J Neuropathol Exp Neurol*. 1981;40:410–427.
32. Cregg JM, Vedvick TS, Raschke WC. Recent advances in the expression of foreign genes in Pichia pastoris. *Biotechnology*. 1993;11:905–910.
33. Scorer CA, Buckholz RG, Clare JJ, Romanos MA. The intracellular production and secretion of HIV-1 envelope protein in the methylotrophic yeast Pichia pastoris. *Gene*. 1993;136:111–119.

34. Combeau C, Didry D, Carlier MF. Interaction between G-actin and myosin subfragment-1 probed by covalent cross-linking. *J Biol Chem*. 1992;267:14038–14046.
35. Van Dijk J, Furch M, Derancourt J, et al. Differences in the ionic interaction of actin with the motor domains of non-muscle and muscle myosin II. *Eur J Biochem*. 1999;260: 672–683.
36. Simm FC, Krietsch WK, Isenberg G. On the interaction of bovine seminal RNase with actin in vitro. *Eur J Biochem*. 1987;166:49–54.
37. Antignani A, Naddeo M, Cubellis MV, Russo A, D'Alessio G. Antitumor action of seminal ribonuclease, its dimeric structure, and its resistance to the cytosolic ribonuclease inhibitor. *Biochemistry*. 2001;40:3492–3496.
38. Matousek J. Ribonucleases and their antitumor activity. *Comp Biochem Physiol C Toxicol Pharmacol*. 2001;129:175–191.
39. Pardridge WM, Nowlin DM, Choi TB, Yang J, Calaycay J, Shively JE. Brain capillary 46,000 dalton protein is cytoplasmic actin and is localized to endothelial plasma membrane. *J Cereb Blood Flow Metab*. 1989;9:675–680.
40. Hu GF, Chang SI, Riordan JF, Vallee BL. An angiogenin-binding protein from endothelial cells. *Proc Natl Acad Sci USA*. 1991;88:2227–2231.
41. Moroianu J, Fett JW, Riordan JF, Vallee BL. Actin is a surface component of calf pulmonary artery endothelial cells in culture. *Proc Natl Acad Sci USA*. 1993;90:3815–3819.
42. Liu Y, Emilion G, Mungall AJ, et al. Physical and transcript map of the region between D6S264 and D6S149 on chromosome 6q27, the minimal region of allele loss in sporadic epithelial ovarian cancer. *Oncogene*. 2002;21:387–399.
43. Fujii T, Tachibana M, Dhar DK, et al. Combination therapy with paclitaxel and thalidomide inhibits angiogenesis and growth of human colon cancer xenograft in mice. *Anticancer Res*. 2003;23:2405–2411.
44. Klauber N, Parangi S, Flynn E, Hamel E, D'Amato RJ. Inhibition of angiogenesis and breast cancer in mice by the microtubule inhibitors 2-methoxyestradiol and taxol. *Cancer Res*. 1997;57:81–86.
45. Xu G, Pan J, Martin C, Yeung SC. Angiogenesis inhibition in the in vivo antineoplastic effect of manumycin and paclitaxel against anaplastic thyroid carcinoma. *J Clin Endocrinol Metab*. 2001;86:1769–1777.
46. Kuttner C, Beecken W-D, Berens A, Eckart A. Paclitaxel administration along with antiangiogenic therapy in HNSCC xenograft model. *Int Poster J Dent Oral Med*. 2001;3: poster 93.
47. Jain RK. Tumor angiogenesis and accessibility: role of vascular endothelial growth factor. *Semin Oncol*. 2002;29:3–9.
48. Ferrara N. Vascular endothelial growth factor: basic science and clinical progress. *Endocrine Rev*. 2004;25:581–611.
49. Ferrara N, Hillan KJ, Novotny W. Bevacizumab (Avastin), a humanized anti-VEGF monoclonal antibody for cancer therapy. *Biochem Biophys Res Commun*. 2005;333:328–335.